Combined inhibition of IL-1, IL-33 and IL-36 signaling by targeting IL1RAP ameliorates skin and lung fibrosis in preclinical models of Systemic Sclerosis

Caitríona Grönberg[1#], Sara Rattik[1#], Cuong Tran-Manh[3/4], Xiang Zhou[3/4], Aleix Rius Rigau[2], Yi-Nan Li[3/4], Andrea-Hermina Györfi[3/4], Emil-Alexandru Matei[3/4], Nicholas Dickel[5], Meik Kunz[5], Alexander Kreuter[6], Honglin Zhu[7], Petter Skoog[1], David Liberg[1], Jörg H.W. Distler[3/4#], Thuong Trinh-Minh[3/4#]

[1] Cantargia AB, Ideon Gateway, Scheelevägen 27, 22363, Lund, Sweden; [2] Department of Internal Medicine 3, University Hospital Erlangen, Erlangen, Germany; [3] Department of Rheumatology, University Hospital Düsseldorf, Heinrich-Heine-University Düsseldorf, Düsseldorf, Germany; [4] Hiller Research Center, University Hospital Düsseldorf, Heinrich-Heine-University Düsseldorf, Düsseldorf, Germany; [5] Chair of Medical Informatics, Friedrich-Alexander University of Erlangen-Nürnberg, Erlangen, Germany; [6] Department of Dermatology, Venereology, and Allergology, HELIOS St. Elisabeth Hospital Oberhausen, University Witten-Herdecke, Witten, Germany; [7] Department of Rheumatology, Xiangya Hospital, Central South University, Changsha, Hunan, China.

# Contributed equally

Corresponding authors:

David Liberg, PhD; Cantargia AB, Ideon Gateway, Scheelevägen 27, 22363, Lund, Sweden; email: david.liberg@cantargia.com

Jörg H.W. Distler, MD; Department of Rheumatology and Hiller Research Center, University Hospital Düsseldorf, Heinrich-Heine-University Düsseldorf, Moorenstr. 5, 40225 Düsseldorf, Germany; Tel.: +49 211 8117817; FAX: +49 211 8116455; email: joerg.distler@med.uni-duesseldorf.de

Grönberg C, *et al. Ann Rheum Dis* 2024;0:1–13. doi: 10.1136/ard-2023-225158

Key words: fibroblasts, fibrosis, inflammation, SSc, IL-1, IL1RAP, IL-33, IL-36

Material and methods

Expression analysis

Microarray data of 11 healthy and 14 systemic sclerosis (SSc) left-arm-derived skin samples from the publicly available SSc dataset GSE59787, which composes of SSc patients from three different cohorts, [1-3] were retrieved from the NCBI Gene Expression Omnibus (GEO) repository. Data were $\log_2$ transformation before differential gene expression (DGE) analysis. The statistics (adjusted p-value) and fold differences of each gene were computed by R package "limma" (version 3.44.3) in RStudio (R version 4.0.2) using the Benjamini-Hochberg correction method. In a confirmatory approach, RNA sequencing data of 26 healthy and 47 systemic sclerosis (SSc) skin samples (GSE130955) were analyzed. In contrast to the previous cohorts, only patients with early diffuse cutaneous SSc (disease duration mean is around 1.3 years) were included and samples were collected in a multicenter effort [4]. The raw paired-end reads were aligned to the GRCh38 reference genome by Spliced Transcripts Alignment to a Reference (STAR) method. After that, the aligned reads were quantified using the "featureCounts" from R package "Rsubread" (version 1.22.2). The trimmed mean of M values method was used for normalization of read count. Next, data were analyzed with the Bioconductor R package "edgeR" in RStudio using the Benjamini-Hochberg method to compute the adjusted p-value of each gene. The RNA levels were visualized as a heatmap plot using "pheatmap" R package (version 1.0.12). The comparisons of target genes between groups were presented as violin plot by using "ggplot2" R package (version 3.3.2).

We also obtained RNA datasets of samples exposed to interleukin (IL)-1β, IL-33, and IL-36γ from the NCBI GEO database with the accession numbers GSE40560, GSE147235, and GSE175732, respectively. GSE40560 included four samples of healthy human dermal fibroblasts stimulated with IL-1β and four non-stimulated controls. GSE147235 contained five

lung samples from mice challenged with IL-33 intranasally and five untreated controls [5]. GSE175732 consisted of three ear samples from mice challenged with IL-36γ intradermally and three untreated controls. We analyzed all data using the same pipelines as outlined for SSc above. To compare mouse and human data and to detect reciprocally expressed genes, we mapped murine orthologues to human gene symbols using the R package "biomaRt" (v 2.48.3).

Image mass cytometry staining

The antibodies used for image mass cytometry (IMC) were acquired preconjugated (Standard Biotools, San Francisco, CA, USA) or in purified preparations (**Supplementary table 1**). All purified antibodies were first validated by standard immunofluorescence staining. Purified antibodies were conjugated to Lanthanide or Indium metals using the Maxpar X8 antibody labeling kit (Standard Biotools) following the manufacturer's instructions. Afterwards, the complete panel was validated again by IMC.

Frozen sections (5µm) were incubated for 1 hour at -20°C in a previously chilled cuvette and at 4°C afterwards. The sections were fixed on ice with 1% PFA for 5 minutes and permeabilized with methanol for 5 minutes. After washing with PBS, the samples were blocked with "SuperBlock" buffer (Thermofischer, 37515) for 1 hour at room temperature. Next, samples were incubated overnight at 4°C with the metal-labeled antibody mix in 0.5% BSA. After washing in PBS-T (PBS and 0.2% Tween 20) and in PBS, iridium-Intercalator (125 µM) was applied at 1/400 for 5 minutes at room temperature for DNA staining, followed by additional washing steps in PBS and in deionized H_2O. Skin samples from five SSc patients and five healthy individuals were stained. Hematoxilin-Eosin staining of consecutive cuts was used to select the area for analysis that encompassed all epidermal and dermal layers of the skin. Imaging was acquired using the Hyperion Imaging System coupled to a Helios mass cytometer

Grönberg C, *et al. Ann Rheum Dis* 2024;0:1–13. doi: 10.1136/ard-2023-225158

(both Standard Biotools) after daily calibration, tuning and quality control. All IMC data were stored as MCD and txt files. The patient information is described in **Supplementary table 2**.

Image mass cytometry data analysis

The stainings were analyzed using the MCD viewer software (Standard Biotools). MCD files were converted to TIFF format and segmented into single cells using a publicly available analysis pipeline [6]. The single cell data (mean expression of all pixels belonging to the same cell and spatial information) was extracted and converted to SpatialExperiment format [7], hyperbolic arcsine (arcsinh) transformed with cofactor 1 and rescaled to values ranging from 0 and 1 with the R package "imcRtools". An isotype antibody was used as control to identify the $IL1RAP^+$ cells. The population of interest ($E\text{-}cadherin^-$; $Isotype^-$; $IL1RAP^+$) was selected and subgrouped into $CD31^+$ and $CD45^-$ (endothelial cells), $CD45^+$ and $CD31^-$ (leukocytes), or $CD45^-$ and $CD31^-$ (mesenchymal) cells by manual gating and spatial reference by FlowJo. Each of these subsets were clustered using the FlowSOM algorithm integrated in the R package "Spectre" and plotted on the cell mask to obtain the spatial reference using the R package "cytomapper" [8]. Afterwards, the frequencies and protein expression levels of each cell population was plotted as pie chart or violin plot using Graphpad Prism 8.0.

Treatment

A mIgG2a LALA-PG mutated anti-mouse IL1RAP antibody (mCAN10), blocking IL-1, IL-33 and IL-36 signaling without activating Fc receptors, was provided by Cantargia AB. A mIgG2a LALA-PG antibody recognizing the hen egg lysosome (HEL) protein was used as isotype control (provided by Cantargia AB). Antibodies were given i.p twice a week, with a first loading dose at 20 mg/kg and the following doses at 10 mg/kg. This dosing regimen has been

established by PK studies in wild type mice (data not shown). Nintedanib was given at 50 mg/kg p.o. daily [9].

Receptor occupancy (RO)

Sixteen C57Bl/6 female mice were treated with monosodium urate (MSU, i.p. 2.5 mg/mouse). MSU was used to increase IL1RAP expression on monocytes and neutrophils in the circulation. Sixteen hours post MSU challenge, blood was collected in EDTA tubes. Blood from 4 mice were pooled giving 4 groups with 4 mice per group, in the following text referred to as 4 donors. All preparations of blood samples for flow cytometry and washing procedures were performed at 4°C. The experiment was performed according to the EU animal welfare standard and was performed at Truly Labs, Lund, Sweden. To assess the potency of unlabeled mCAN10 antibody, serial dilutions of mCAN10 were prepared in PBS with 1% BSA aiming for the following final concentrations in blood mixture: 0,1 to 250 µg/ml. Aliquots were mixed with 50µl of whole blood and preincubated at 4°C for 1 h. For control wells, PBS with 1% BSA was mixed with 50 µl of whole blood to generate the background samples (0% inhibition) and for 100% inhibition, cells were stimulated with high dose of unlabeled mCAN10 (250 µg/ml).

Subsequently, blood was stained for 30min at 4°C with Ly6C (PE, clone HK1.4, 128008, BioLegend), SiglecF (PE/CF594, clone: E50-2440, 562757, BD Biosciences), Ly6G (BV650, clone: 1A8, 127641, BioLegend), Viability dye v500 (L34965, Invitrogen) and 20µg/ml mCAN10 (conjugated in-house to AF647) or 20µg/ml isotype controls (conjugated in-house to AF647). Erythrocytes were lysed with BD lysing solution (349202, BD Biosciences, Thermo Fisher Scientific) for 4x2min.

Finally, cells were washed with PBS with 1%BSA and fixed in 1xCellFix (340181, BD Biosciences, Thermo Fisher Scientific). Samples were analyzed on CytoFlex (Beckman

Coulter). To correct for fluorescence spillover compensation with compensation beads was performed before the sample run (ArC Amine Reactive compensation beads for viability dye (A10346, Life Technologies) and UltraComp eBeads for the fluorescent antibodies (01-3333-41, Invitrogen)).

Average Mean fluorescence intensity (MFI) of isotype control for a specific donor was subtracted from MFI of each sample from the equivalent donor. Using beneath formula, data was converted into percentage format, with the 0% inhibition controls set as 0:

((MFI (no unlabeled mCAN10) – MFI (sample X))/MFI (no unlabeled mCAN10))*100

Data were analyzed in Graph Pad Prism 7.0 and EC50 values were generated using non-linear regression fit model ([Agonist] vs. response -- Variable slope (four parameters) with default Fitting method - Least squares regression.

Immunofluorescence staining

Formalin-fixed, paraffin-embedded skin sections were stained with primary antibodies against IL-1β (P420B, Thermo Fisher Scientific, 1:100 dilution), IL-33 (AF3625, Biotechne, R&D Systems, 1:100 dilution), or IL-36γ (orb537665, Biorbyt, 1:100 dilution). Nuclei were counterstained using DAPI (Santa Cruz Biotechnology, Heidelberg, Germany). Alexa Fluor®488 donkey anti-rabbit or Alexa Fluor®488 donkey anti-mouse (Life Technologies, California, USA, 1:200 dilution) were used as secondary antibodies. The staining was analyzed with Axio Observer 7 microscope (ZEISS, Jena, Germany).

Quantification of extra cellular matrix deposition

Extra cellular matrix (ECM) staining was performed as described previously [10]. Dermal fibroblasts from SSc patients ($2x10^4$ per well for 96-well plates) were seeded on each well of dark-walled imaging plates (BD Biosciences). The cells were preincubated with anti-IL1RAP antibody (CAN10) or isotype control antibody at the concentration of 50 ng/mL for one hour prior to the stimulation of DPBS, TGFβ (final concentration at 10 ng/mL), combination of IL-1β/IL-33/IL-36γ (abbreviated as ILs, including final concentration of IL-1β at 1 ng/mL, IL-33 at 100 ng/mL, and IL-36γ at 100 ng/mL), or mixture of ILs and TGFβ, for 48 hours. Cells were lysed with 0.25 M ammonium hydroxide in 25 mM Tris for 1 minute at 37ºC. The ECM was washed 3 times in DPBS, fixed by 100% methanol for 20 minutes at -20ºC, and then stained with anti-fibronectin Alexa Fluor®488 (eBiosciences; 1:200), and anti-type I collagen antibody (AB745, Millipore; 1:200). The ECM images were scanned by using the CellInsight CX5 High Content Screening platform (Thermo Fisher Scientific) and were automatically quantified the average intensity per well using a custom pipeline in HCS Studio Cell Analysis software.

Quantification of myofibroblast marker

Dermal fibroblasts from SSc patients ($2x10^3$ per well) were seeded on each well of 96-well plate (Greiner Bio-One). The cells were preincubated with anti-IL1RAP antibody (CAN10) or isotype control antibody at the concentration of 50 ng/mL for one hour prior to the stimulation of DPBS, TGFβ (final concentration at 10 ng/mL), combination of IL-1β/IL-33/IL-36γ (abbreviated as ILs, including final concentration of IL-1β at 1 ng/mL, IL-33 at 100 ng/mL, and IL-36γ at 100 ng/mL), or mixture of ILs and TGFβ, for 48 hours. Cells were fixed with 4% para-formaldehyde for 10 minutes at room temperature, and then stained with anti-αSMA antibody (MA5-11547, Thermo Fisher Scientific, 1:1000 dilution). The cell images were scanned by using the CellInsight CX5 High Content Screening platform (Thermo Fisher

Scientific) and were automatically quantified the average intensity per well using a custom pipeline in HCS Studio Cell Analysis software.

Mouse models of fibrosis

Three complementary mouse models of dermal and pulmonary fibrosis of SSc were employed:

Murine sclerodermatous chronic graft-versus-host disease (cGvHD)

The B10.D2→Balb/c (H-2(d)) minor histocompatibility antigen-mismatched model was performed as described [11, 12]. Briefly, female BALB/c (H-2d) mice were purchased from Janvier (Le Genest St. Isle, France). Male B10.D2 (H-2d) mice were purchased from Jackson Laboratory (Bar Harbor, ME). All mice were maintained in specific pathogen-free conditions with sterile pellet food and water and a normal day-night cycle. For isolation of unfractioned bone marrow cells, tibial and femoral bones were prepared under sterile conditions. Phosphate buffered saline (PBS) was used to flush bone marrow cells from bone marrow cavities. Subsequently, bone marrow cells were filtered through 70 µm nylon meshes (BD Biosciences, Heidelberg, Germany) followed by erythrocyte hemolysis. The remaining bone marrow cells were kept on ice until transplantation. Transplantation of bone marrow cells and splenocytes was performed as follows: Recipient mice (BALB/c (H-2d)) with an age of 8 weeks received total body irradiation with 700 cGy. Six hours after irradiation, all BALB/c (H-2d) recipients received bone marrow from either BALB/c (H-2d) in a syngeneic or B10.D2 (H-2d) in an allogeneic transplantation manner. For transplantation, 5 x 10^6 splenocytes and 2 x 10^6 bone marrow cells from donor mice were resuspended in 0.2 ml of PBS and injected via tail veins [12]. To reflect the clinical situation with treatment only upon clinical signs of cGvHD, treatment was started 21 days after bone marrow transplantation and thus after the first

clinically detectable manifestations of cGvHD in allogeneically transplanted mice. The outcome of treatment was analyzed seven weeks after transplantation. Ten mice per group were analyzed. All studies were performed according to the EU animal welfare standard.

Bleomycin-induced dermal fibrosis

Skin fibrosis was induced by daily subcutaneous injections of bleomycin (bleo, 2.5 mg/kg, Sigma-Aldrich) in defined and marked areas of the upper back (1 cm^2) for up to six weeks as described [13, 14]. Treatment was initiated after three weeks of pre-challenge with bleomycin. The outcome was analyzed three weeks after the first injection of bleomycin (six weeks after the first bleomycin-injection. The outcome was analyzed six weeks after the first bleomycin-injection. Ten mice per group were analyzed.

Topoisomerase I (topo)-induced dermal fibrosis

In the topo-model, fibrosis was induced in five weeks old C57Bl/6 mice by subcutaneous injections of 500 U/mL recombinant DNA topoisomerase I mixed 3:2 with complete Freund's adjuvant (CFA, Sigma) [15, 16]. Mice were injected every other week and the outcome was analyzed after eight weeks. Mice treated with equal volumes of CFA served as controls. Treatment with initiated two weeks after the first topo-injection. The outcome was analyzed eight weeks after the first topo-injection. Ten mice per group were analyzed.

General monitoring

Mice were monitored clinically on a daily basis for behavior, activity, texture of the fur and consistency of the stool. After sacrifice, a gross macroscopic evaluation of the lungs and the skin was performed. All studies were performed according to the EU animal welfare standard. The studies have been approved by the local animal welfare committee of the Government of Mittelfranken, Unterfranken or North-Rinne-Westphalia.

Clinical score of cutaneous cGvHD

Recipient mice were clinically monitored once daily from the day of transplantation to the indicated days after transplantation to determine the incidence and severity of cutaneous cGvHD as well as mobility, diarrhea and weight loss [12, 17]. The following scoring system for cutaneous cGvHD was used: healthy appearance = 0; skin lesions with alopecia < 1 cm^2 in area = 1; skin lesions with alopecia 1 - 2 cm^2 in area = 2; skin lesions with alopecia > 2 cm^2 in area = 3. Incidence was expressed as the percentage of mice that showed clinical manifestations.

Histological evaluation of dermal and pulmonary fibrosis

Skin samples of defined areas of 1 cm^2 on the upper back were fixed in 4 % formalin for 6 h and embedded in paraffin. Five µm sections were cut and stained with hematoxylin and eosin. The dermal thickness was quantified on HE-stained sections using images captured with a light microscope (Nikon eclipse 80i) at 100-fold magnification by manually measuring the distance between the epidermal-dermal junction and the dermal-subcutaneous fat junction at four sites per mouse [18, 19]. Lung samples (right lobes) were fixed in 4 % formalin for 6 h and embedded in paraffin. Five µm sections were cut and stained with Trichrome and Sirius Red. Histologic readouts were evaluation of the fibrotic area as percent of total lung area in Sirius Red stained sections and quantification of pulmonary histological changes using the Ashcroft score [20, 21].

Hydroxyproline assay

The amount of collagen protein in skin and lung samples was determined via hydroxyproline assay [22, 23]. After digestion in 6 M HCl for three hours at 120 °C, the pH of the samples was adjusted to 6 with 6 M sodium hydroxide (NaOH). Afterwards, 0.06 M chloramine T was added to each sample and incubated for 20 min at room temperature. Next, 3.15 M per-chloric acid and 20 % p-dimethylaminobenzaldehyde were added and samples were incubated for additional 20 min at 60 °C. The absorbance was determined at 557 nm with a Spectra MAX 190 microplate spectrophotometer. Absolute values were determined using standard curved generated with type I collagen (Sigma Aldrich).

Detection of myofibroblasts

Myofibroblasts are characterized by the expression of α-smooth muscle actin (αSMA). Fibroblasts positive for αSMA were detected by incubation with monoclonal anti-αSMA antibodies (clone 1A4, Sigma-Aldrich, Steinheim, Germany). The expression was visualized with horseradish peroxidase labeled secondary antibodies and 3,3-diaminobenzidine tetra hydrochloride (DAB) (Sigma-Aldrich). Monoclonal mouse IgG antibodies (Calbiochem, San Diego, CA, USA) were used for controls. Images of sections stained for αSMA were captured on a light microscope (Nikon eclipse 80i). Images were manually evaluated at four different areas at 200-fold magnification. Myofibroblasts were defined as αSMA-positive, single, spindle-shaped cells in the dermis [24, 25].

Bioinformatical analyses

RNASeq preprocessing and analysis

Raw paired-end reads were trimmed of low quality region and adapter contamination by using TrimGalore function in trimming tool FastQC (version 0.6.4). The trimmed reads were aligned to GRCm39 reference genome by Spliced Transcripts Alignment to a Reference (STAR) method afterward. Next, the aligned reads were quantified using the "featureCounts" from R package "Rsubread" (version 1.22.2). Principal component analysis (PCA) was performed to determine the potential outliners among samples in each batch. Following PCA, three samples (one per condition) were excluded. For each group, four samples resulting in dense group-specific clustering were selected. data were analyzed with the Bioconductor R package "edgeR" in RStudio using the Benjamini-Hochberg correction method to compute the adjusted p-value of each gene. The significant DEGs list is considered as adjusted p-value ≤ 0.05 and $|\log_2 FC| \geq 1.5$ for the comparison between allogenically-transplanted mice and mice with syngeneic transplantation, and as adjusted p-value ≤ 0.05 and $|\log_2 FC| \geq 1$ for the comparison between allogenically-transplanted mice treated with mCAN10 and allogenically-transplanted mice. The results were visualized as Volcano plot by using the "EnhancedVolcano" package (version 1.10.0) according to the $\log_2 FC$ and –log10adjusted-p-value of DEGs. Hierarchical cluster analyses were performed using "pheatmap" package (version 1.0.12). Overrepresentation analysis (ORA) was performed using the "g:Profiler" web-server with Benjamini-Hochberg as the computation method to calculate adjusted p-value for Gene Ontology – biological processes functional terms. The results of ORA were visualized with R package "ggplot2" (v 3.3.5). Gene Set Enrichment Analysis (GSEA) on normalized gene counts was performed using Fast GSEA (fgsea) in R package "clusterProfiler" (version 4.8.3). Venn Diagrams created from BioVenn website represented all possible relations among different DEGs list.

Bioinformatic analysis of the expression of IL1RAP related signaling molecules in bleomycin-induced skin fibrosis

Raw count data of public dataset GSE132869 were retrieved from the NCBI Gene Expression Omnibus (GEO) repository. Data of skin samples from mice injected with bleomycin (n = 8) or with PBS (n = 8) for 14 or 28 days were used for the expression analysis. The raw count was normalized with trimmed mean of M-values (TMM) method from 'edgeR' package (version 3.34.1) in Rstudio (R version 4.1). The DGE was performed by using R package "edgeR" in RStudio with the Benjamini-Hochberg correction method to compute the adjusted p-value of each gene. The RNA levels of target genes including *Il1f6* (Il36α), *Il1f8* (Il36β), *Il1f9* (Il36γ), *Il1rl1* (Il33r/St2), *Il1rl2* (Il36r), *Il1a*, *Il1b*, *Il1r1*, *Il1r2*, *Il1rn*, *Il1rap*, *Il33*, and *Il36* in bleomycin-challenged mice or PBS-treated controls were visualized as heatmaps plot using R package "pheatmap". The comparisons of target genes between groups were presented as box plot by using GraphPad Prism (version 8.3.0).

Inhibition of the stimulatory effects of IL-1 family cytokines by anti-IL1RAP antibody in human dermal fibroblasts and endothelial cells

CAN10, a humanized monoclonal LALA-mutated IgG1κ antibody targeting human IL1RAP, was added at a concentration of 20 µg/mL for 0.5 to 1 hour before stimulating dermal human fibroblasts (normal human dermal fibroblasts, Lonza) or primary human umbilical cord endothelial cells (HUVEC, ATCC). Fibroblast were stimulated with IL-1α (0.1 ng/mL), IL-1β (0.1 ng/mL), IL-36β (150 ng/mL), or IL-36ɣ (150 ng/mL), and HUVECs were stimulated with IL-1α (5 ng/mL), IL-1β (10 ng/mL), IL-33 (30 ng/ml), IL-36α (100 ng/ml), IL-36β (100 ng/ml), or IL-36ɣ (100 ng/ml). Protein analysis for fibroblasts was performed using the LUMINEX platform (Invitrogen) 48 hours after stimulation. Protein analysis from HUVEC for IL-6 and

IL-8 ELISA (human IL-6/IL-8 Duo set R&D Systems, Cat DY206 and DY208) was performed 24 hours after stimulation.

Statistics

All data are presented as mean ± SEM with individual values displayed as dots. Differences between the groups were tested for their statistical significance by One-way-ANOVA. P-values less than 0.05 were considered significant. P-values are expressed as follows: $0.05 > p > 0.01$ as *; $0.01 > p > 0.001$ as **; $p < 0.001$ as *** as compared to pretreatment levels in control mice.

Patient and Public Involvement

Patients or the public were not involved in the design, or conduct, or reporting, or dissemination plans of our research.

Supplementary figure

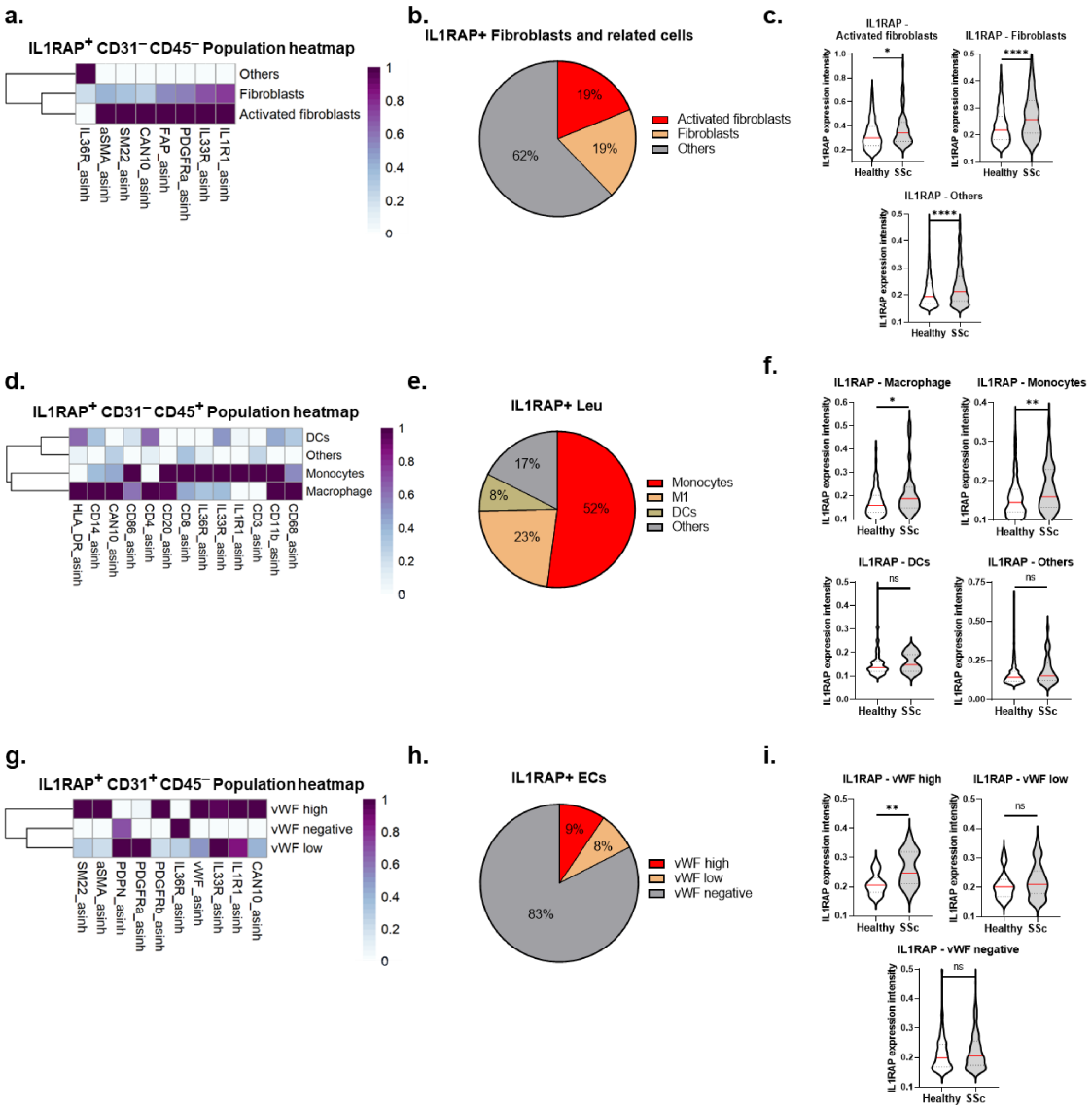

Supplementary figure 1. Expression of IL1RAP in different subpopulations of leukocytes, fibroblasts and endothelial cells by IMC staining. a-c: Fibroblasts and mesenchymal cells (IL1RAP$^+$, CD31$^-$, CD45$^-$): (a) Heatmap illustrating the expression of markers of IL1RAP positive subpopulations of fibroblasts. (b) Proportions of IL1RAP positive subpopulations. (c) Violin plot representing the distribution of the IL1RAP intensity in fibroblast subpopulations. **d-f: Leukocytes (Leu, IL1RAP$^+$, CD31$^-$, CD45$^+$):** (d) Heatmap illustrating the expression of

markers of IL1RAP positive subpopulations of leukocytes. (e) Proportions of IL1RAP positive subpopulations. (f) Violin plot representing the distribution of the IL1RAP intensity in Leu subpopulations. **g-i: Endothelial cells (ECs, IL1RAP^{+}, CD31^{+}, CD45^{-}):** (g) Heatmap illustrating the expression of markers of IL1RAP positive subpopulations of endothelial cells. (h) Proportions of IL1RAP positive subpopulations. (i) Violin plot representing the distribution of the IL1RAP intensity in EC subpopulations. The red line indicates median of data. The statistical significance was determined by two-tailed Mann-Whitney U-test. * indicates significant differences between SSc and healthy control. *: p- value < 0.05; **: p- value < 0.01; ***: p- value < 0.001; and ****: p- value < 0.0001.

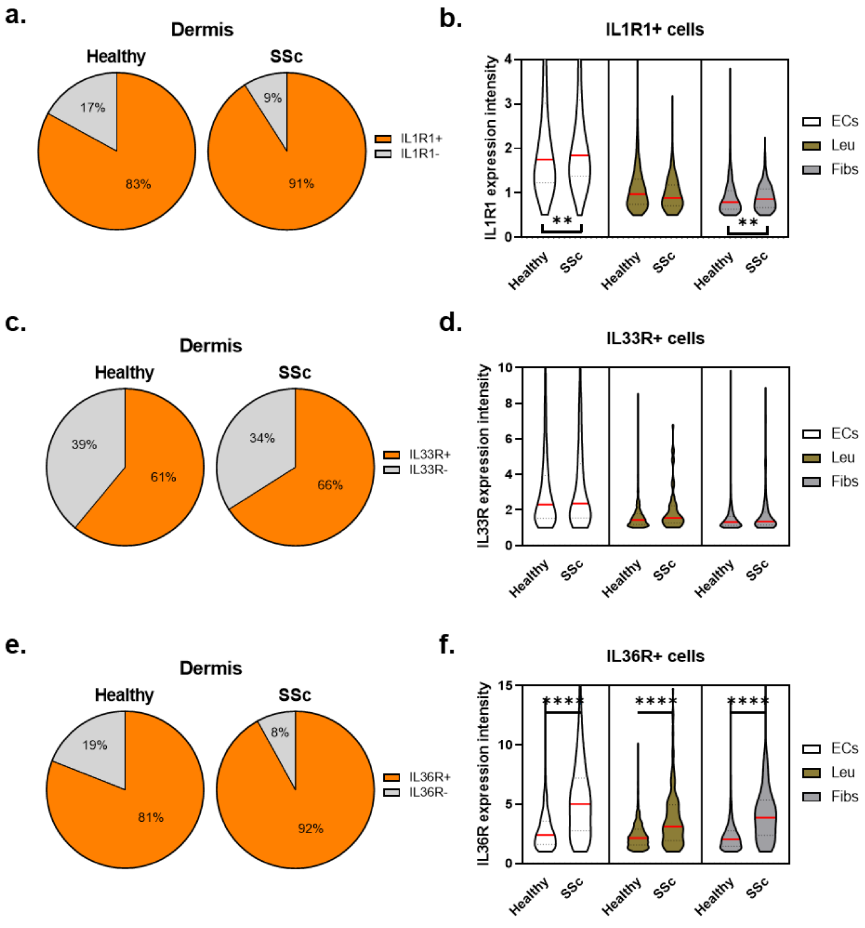

Supplementary figure 2. Expression levels of IL1R1, IL33R and IL36R in SSc and healthy dermis. (a-b) Expression levels of IL1R1: (a) Percentage of positive cells. (b) Violin plot representing the distribution of the IL1R1 intensity on all IL1R1 positive ECs, leukocytes and fibroblasts. **(c-d) Expression levels of IL33R:** (c) Percentage of positive cells. (d) Violin plot representing the distribution of the IL33R intensity on all IL33R positive ECs, leukocytes and fibroblasts. **(e-f) Expression levels of IL36R:** (e) Percentage of positive cells. (f) Violin plot representing the distribution of the IL36R intensity on all IL36R positive ECs, leukocytes and fibroblasts. The red line indicates median of data. The statistical significance was determined by two-tailed Mann-Whitney U-test. * indicates significant differences between SSc and healthy control. *: p- value < 0.05; **: p- value < 0.01; ***: p- value < 0.001; and ****: p-value < 0.0001.

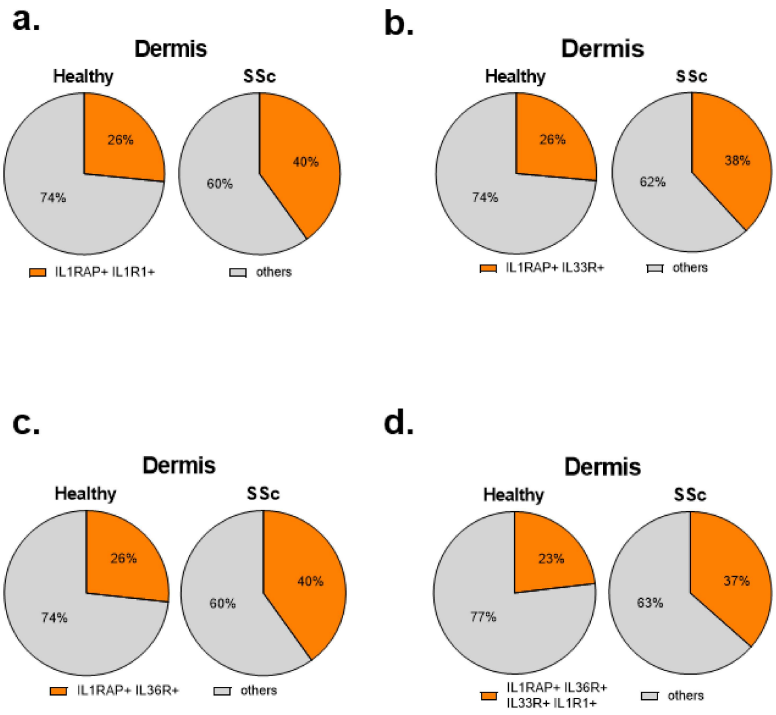

Supplementary figure 3. Coexpression of IL1RAP and IL1R1, IL33R and IL36R in SSc and healthy skin. The percentage of double positive cells of IL1RAP and IL1R1 (a), of IL1RAP and IL33R (b), of IL1RAP and IL36R (c), and of cells positive for IL1RAP, IL1R1, IL33R and IL36R (d) in dermis of SSc patients or healthy donors.

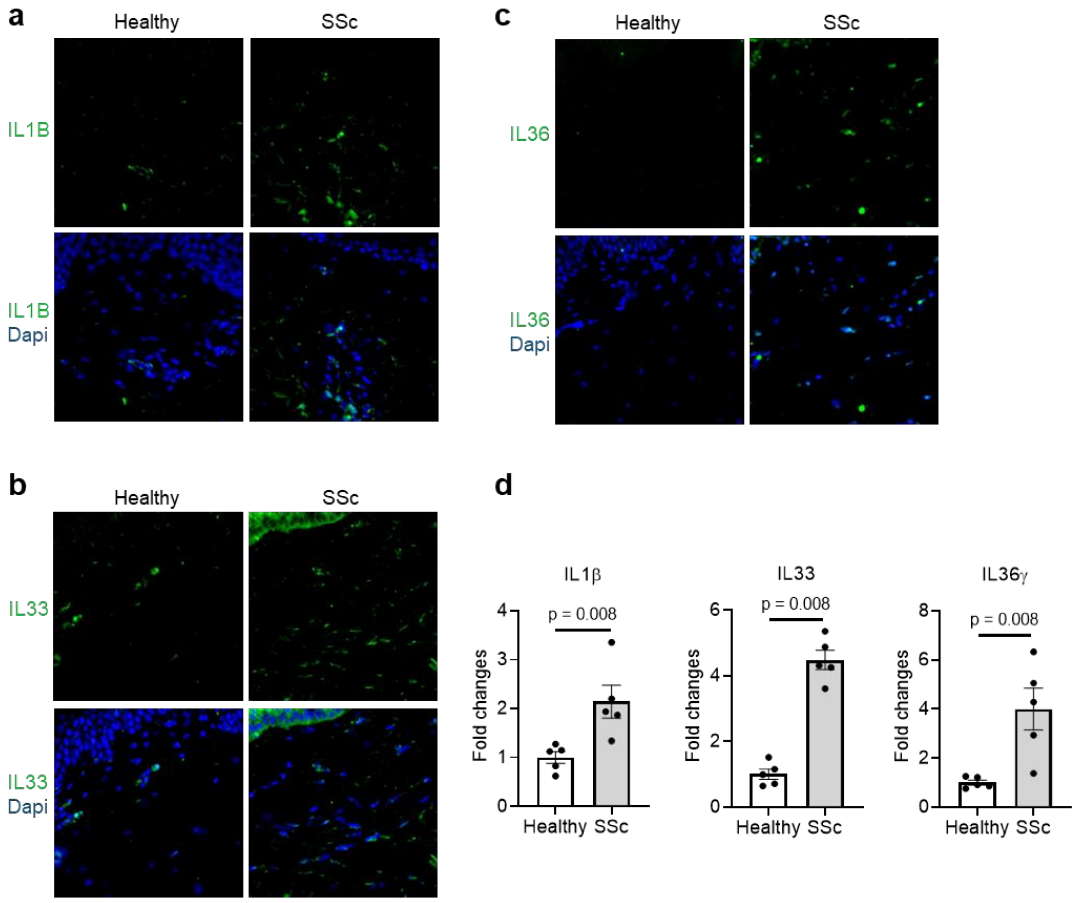

Supplementary figure 4. Protein levels of IL-1β, IL-33, and IL-36γ in the skin of SSc patients and healthy donors. Representative immunofluorescence staining of IL-1β (a), IL-33 (b), or IL-36γ (c) (n = 5 per group) and quantification of intensity of those signals (d). Data are shown as mean ± S.E.M with individual data points. The statistical significance was determined by two-tailed Mann-Whitney *U*-test.

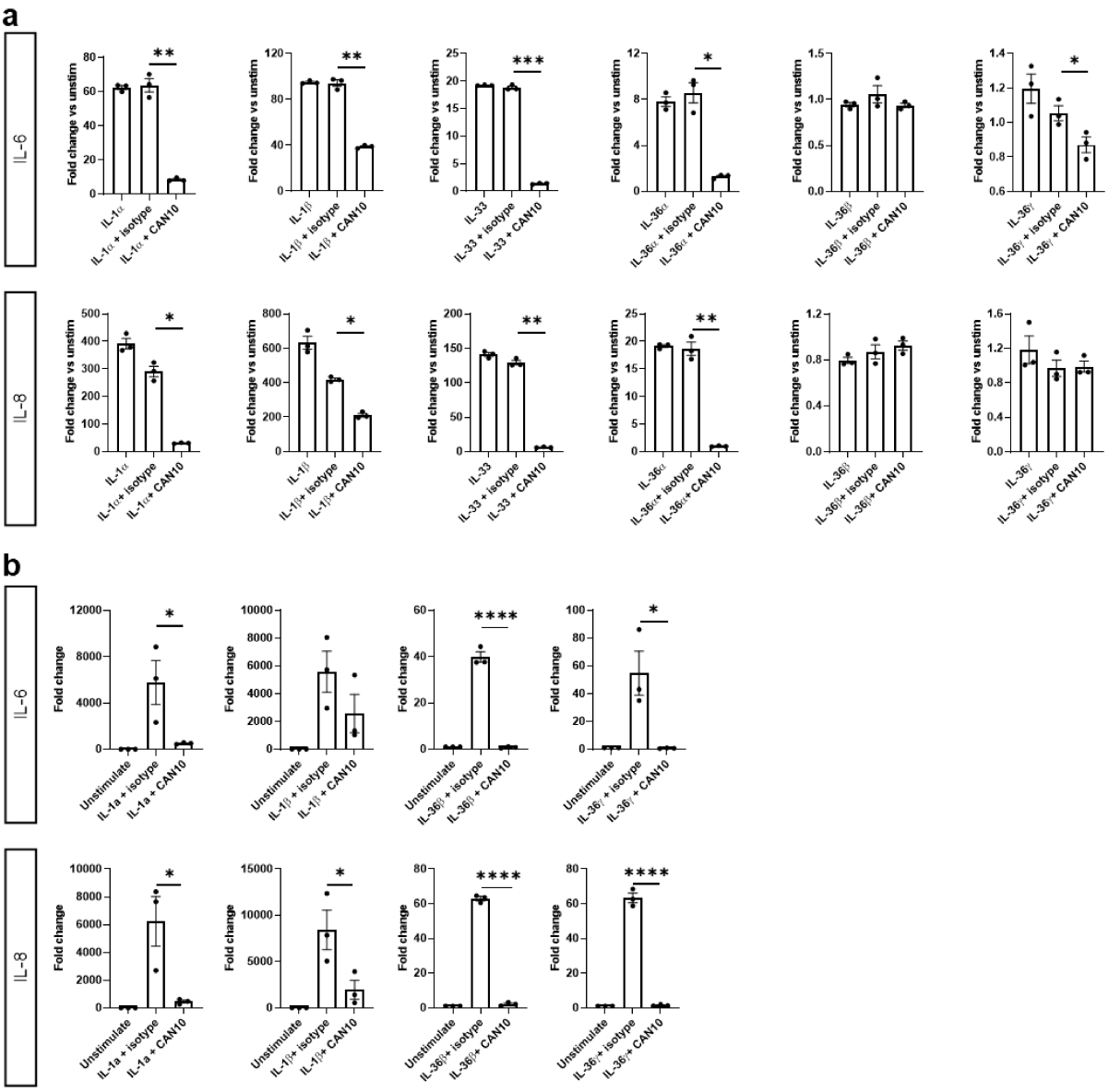

Supplementary figure 5. IL1RAP blockade by CAN10 inhibits IL-1, IL-33 and IL-36 signaling *in vitro*. IL-6 and IL-8 protein levels released by (a) human endothelial umbilical cord cells or (b) by human dermal fibroblasts stimulated with IL-1, IL-33 or IL-36 with or without CAN10 antibody or isotype control antibody (n = 3). Data are shown as mean ± S.E.M with individual data points. The statistical significance was determined by one-way ANOVA with Dunnett's multiple comparison test. * indicates significant differences between syngeneic

group and allogeneic group. *: p-adjusted value < 0.05; **: p-adjusted value < 0.01; ***: p-adjusted value < 0.001; and ****: p-adjusted value < 0.0001.

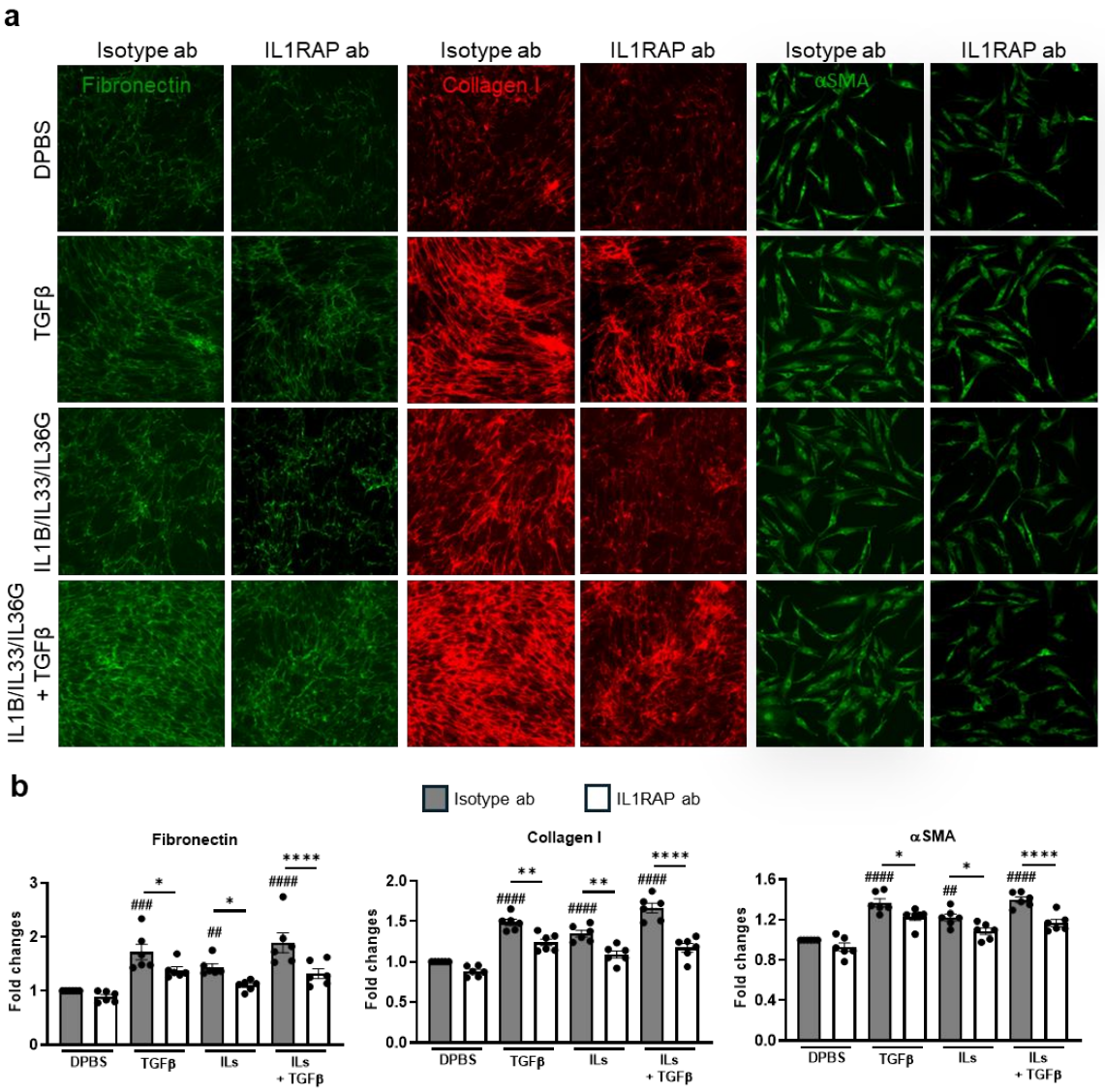

Supplementary figure 6. The impact of the CAN10 antibody on the extracellular matrix deposition and myofibroblast differentiation of fibroblasts stimulated with TGFβ and/or combination of IL-1β, IL-33, and IL-36γ. Staining (a) and quantification (b) of fibronectin and collagen type I deposition, and αSMA expression of fibroblasts isolated from SSc patients (n = 6 donors) stimulated with TGFβ and/or combination of IL-1β, IL-33, and IL-36γ (ILs),

treated with the anti-IL1RAP antibody CAN10 or isotype control antibody. Data are shown as mean ± S.E.M with individual data points. The statistical significance was determined by two-way ANOVA with Tukey's multiple comparison test. # indicates differences of cytokines stimulated fibroblasts compared to DPBS stimulated fibroblasts pretreated with isotype control antibody. * indicates differences of fibroblasts treated with the CAN10 antibody and fibroblasts treated with isotype control, at the same stimulus. # and *: Padj < 0.05; ## and **: Padj < 0.01; ### and ***: Padj < 0.001; #### and ****: Padj < 0.0001.

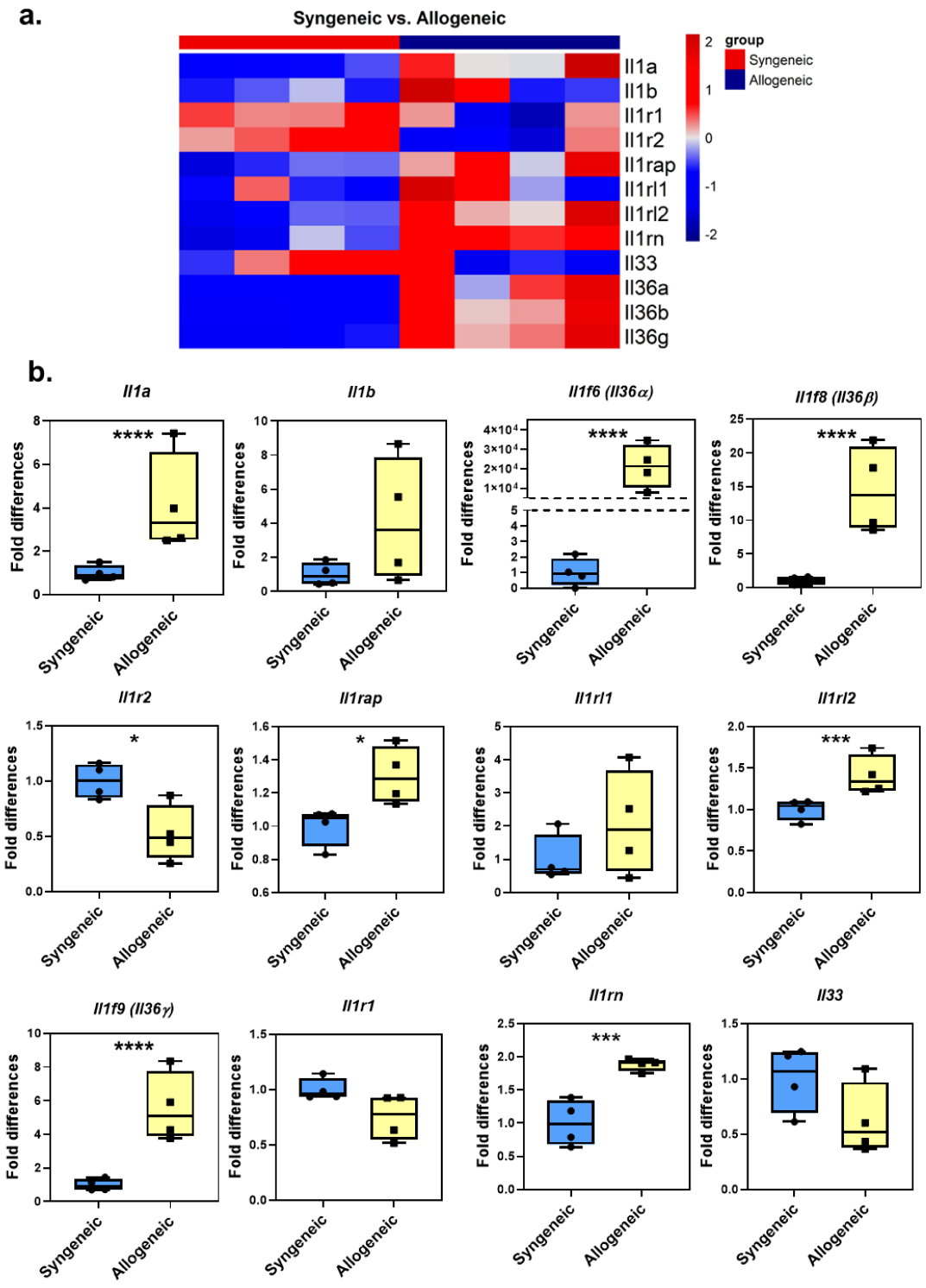

Supplementary figure 7. The expression levels of molecules associated with IL1RAP related signaling in murine sclerodermatous cGvHD. (a) Representative heatmap of mRNA

levels of genes associated with IL1RAP related signaling between syngeneic and allogeneic skin samples. (b) The comparisons of detectable IL1RAP related genes between syngeneic group and allogeneic group, seven weeks after transplantation. * indicates significant differences between syngeneic group and allogeneic group. *: p-adjusted value < 0.05; **: p-adjusted value < 0.01; ***: p-adjusted value < 0.001; and ****: p-adjusted value < 0.0001. *Il1f6*, *Il1f8*, *Il1f9* and *Il1rl1* are commonly recognized as *Il36α*, *Il36β*, *Il36γ* and *Il33r*/St2, respectively.

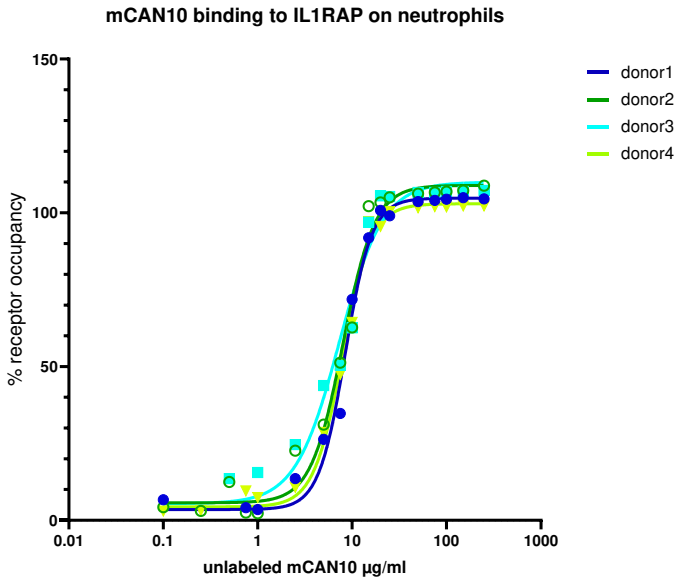

	donor1	donor2	donor3	donor4
EC50	8.454	7.991	7.291	7.945

Supplementary figure 8. Receptor occupancy of the mCAN10 antibody to IL1RAP on neutrophils in whole blood. Blood was taken from MSU-treated mice and a titration with unlabelled mCAN10 was done. A fixed concentration of AF647-labelled mCAN10 was added to the samples and flow cytometry was used to calculate the receptor occupancy (RO) based on the mean fluorescence intensity–of mCAN10-AF647 binding to IL1RAP on Ly6G+ neutrophils in blood.

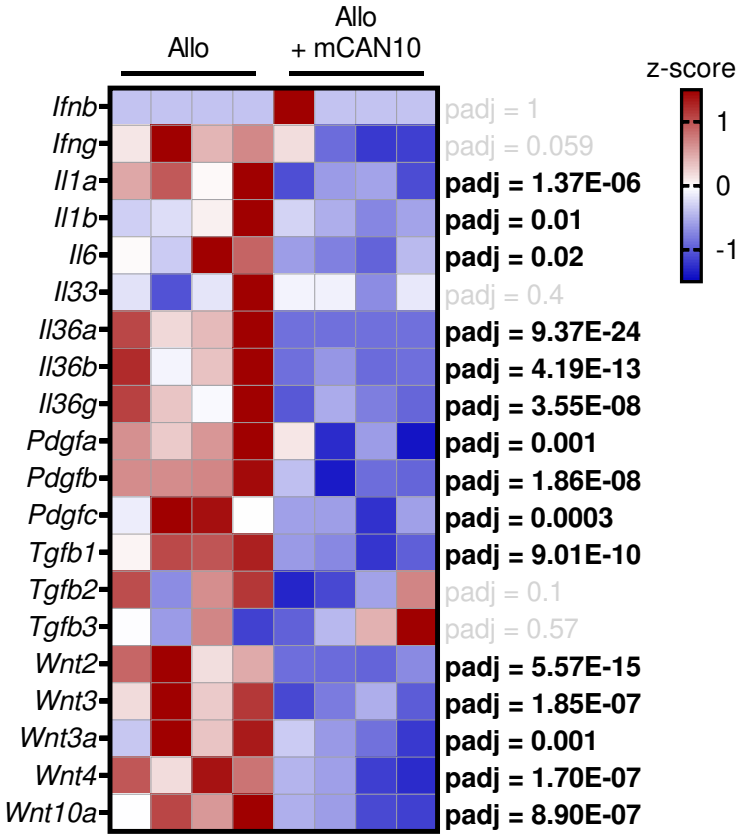

Supplementary figure 9. Expression levels of profibrotic mediators in allogenically-transplanted mice treated with anti-IL1RAP (mCAN10) antibody or isotype control antibody.

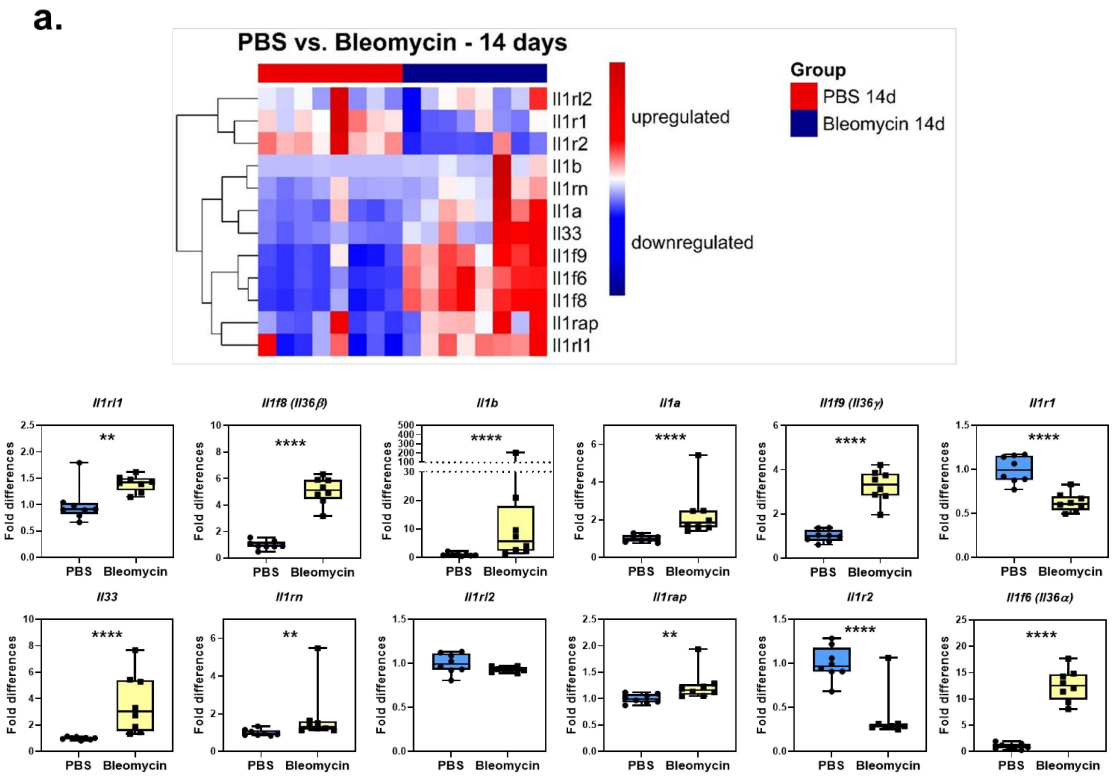
a.
PBS vs. Bleomycin - 14 days
Il1rl2
Il1r1
Il1r2
Il1b
Il1rn
Il1a
Il33
Il1f9
Il1f6
Il1f8
Il1rap
Il1rl1
upregulated
downregulated
Group
PBS 14d
Bleomycin 14d
Il1rl1
Il1f8 (Il36β)
Il1b
Il1a
Il1f9 (Il36γ)
Il1r1
Il33
Il1rn
Il1rl2
Il1rap
Il1r2
Il1f6 (Il36α)
Fold differences
PBS
Bleomycin

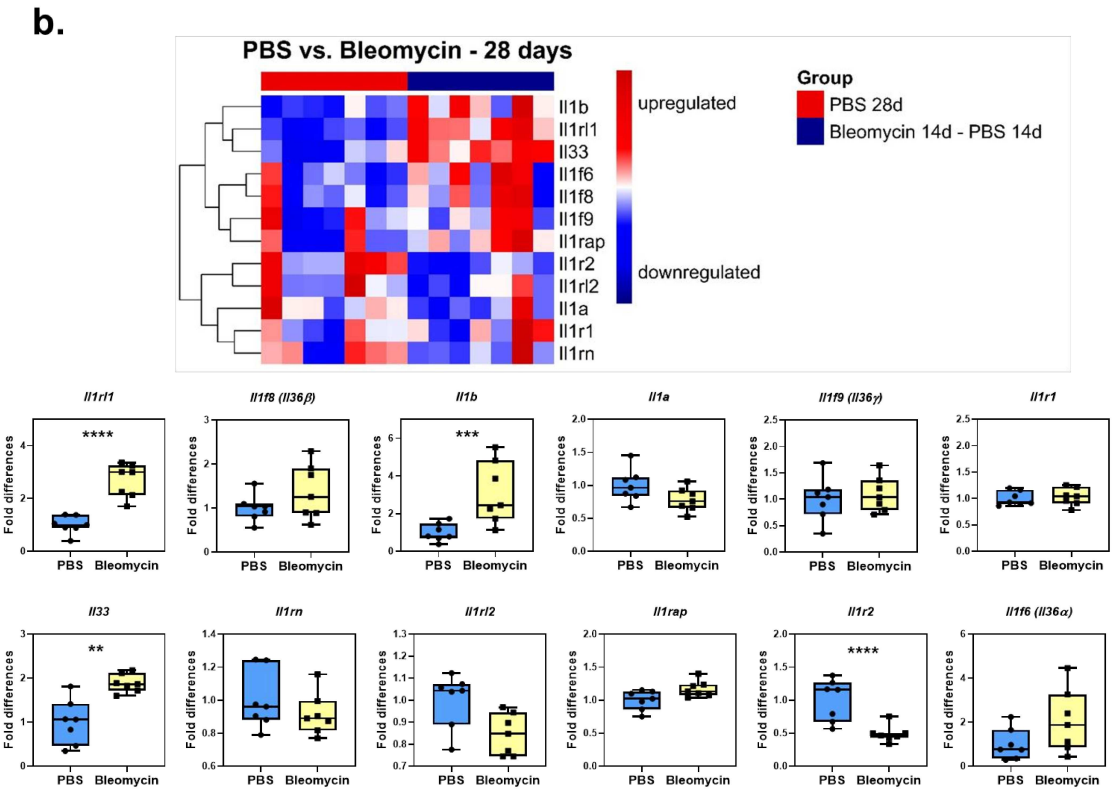
b.
PBS vs. Bleomycin - 28 days
Il1b
Il1rl1
Il33
Il1f6
Il1f8
Il1f9
Il1rap
Il1r2
Il1rl2
Il1a
Il1r1
Il1rn
upregulated
downregulated
Group
PBS 28d
Bleomycin 14d - PBS 14d
Il1rl1
Il1f8 (Il36β)
Il1b
Il1a
Il1f9 (Il36γ)
Il1r1
Il33
Il1rn
Il1rl2
Il1rap
Il1r2
Il1f6 (Il36α)
Fold differences
PBS
Bleomycin

Supplementary figure 10. Expression of genes associated with IL1RAP related signaling in the mouse model of bleomycin-induced skin fibrosis using data from NCBI/GEO/GSE132869. (a) 14 days of bleomycin-challenge. (b) 14 days of bleomycin-challenge followed by 14 days of injections with the solvent NaCl. Mice injected with NaCl throughout the observation period served as controls. Shown are representative heatmaps of mRNA expression level of target genes along with box plots for the individual genes. * indicates significant differences between bleomycin challenged group and PBS treated group. *: p-adjusted value < 0.05; **: p-adjusted value < 0.01; ***: p-adjusted value < 0.001; and ****: p-adjusted value < 0.0001. *Il1f6*, *Il1f8*, *Il1f9* and *Il1rl1* are commonly recognized as *Il36α*, *Il36β*, *Il36γ* and *Il33r*/St2, respectively.

Supplementary table 1. List of antibodies used in IMC experiment

Metal	Antigen	Clone	Company
115In	TPSAB1	AA1	Biolegend
141Pr	HLA-DR	LN3	Biolegend
144Nd	CD14	EPR3653	Standard Biotools
145Nd	CD31	Policlonal	R&D
146Nd	SM22	polyclonal	Abcam
148Nd	PDGFRa	Poli Goat	R&D
150Nd	a-SMA	1A4	Sigma
151Eu	PDGFRb	18A2	Biolegend
152Sm	CD45	D9M8I	Standard Biotools
153Eu	IL1RAP	CAN10	Cantargia
155Gd	CD86	Polyclonal	R & D
156Gd	CD4	EPR6855	Standard Biotools
158Gd	E-Cadherin	24E10	Standard Biotools
161Dy	CD20	2H7	Standard Biotools
162Dy	CD8	C8/144B	Standard Biotools
163Dy	Collangen	EPR7785	abcam
164Dy	IL36R	n/a	Cantargia
165Ho	vWillebrand	Poli Rb	Merck

Metal	Antigen	Clone	Company
166Er	IL33R	n/a	Cantargia
168Er	IL1R1	Polyclonal	R & D
169Tm	Isotype	Isotype control for CAN10	Innovagen
170Er	CD3	Poly C-Terminal	Standard Biotools
172Yb	CD11b	M1/70	R&D
173Yb	Podoplanin	LpMab-21	Biolegend
174Yb	FAP	Poli Sheep	R&D
175Lu	CD68	KP1	Biolegend
176Yb	Histone-3	D1H2	Standard Biotools
191Ir	Ir		Standard Biotools
195Pt	Segmentation kit (ICSK1)		Standard Biotools
196Pt	Segmentation kit (ICSK2)		Standard Biotools
198Pt	Segmentation kit (ICSK3)		Standard Biotools

Supplementary table 2. Demographic clinical data of internal cohort.

Parameter	
Number of patients (n)	4
female gender (%)	100
mean age (SD) (years)	62 (3.5)
mean disease duration (SD) (years)	15 (13.5)
mean global mRSS (SD)	11.5 (6.5)
mean local mRSS (SD)	1.0 (0.0)
dcSSc (%)	50
ATA (%)	50
ACA (%)	0
ARA (%)	50
SSc-ILD (%)	0

PAH (%)	50
Mycophenolate mofetil (%)	50
Nintedanib (%)	0
Tocilizumab (%)	0
Rituximab (%)	0
Methotrexate (%)	0

mRSS=modified Rodnan skin score; dcSSc=diffuse cutaneous systemic sclerosis; ATA=anti-topoisomerase I antibodies; ACA=anti-centromere antibodies; ARA=anti-RNA polymerase III antibodies; SSc-ILD=systemic-sclerosis-associated interstitial lung disease; SSc-PAH=systemic-sclerosis-associated pulmonary arterial hypertension.

References

1. Milano A, Pendergrass SA, Sargent JL, George LK, McCalmont TH, Connolly MK, et al. Molecular subsets in the gene expression signatures of scleroderma skin. PLoS One. 2008 Jul 16; 3(7):e2696.
2. Pendergrass SA, Lemaire R, Francis IP, Mahoney JM, Lafyatis R, Whitfield ML. Intrinsic gene expression subsets of diffuse cutaneous systemic sclerosis are stable in serial skin biopsies. J Invest Dermatol. 2012 May; 132(5):1363-1373.
3. Hinchcliff M, Huang CC, Wood TA, Matthew Mahoney J, Martyanov V, Bhattacharyya S, et al. Molecular signatures in skin associated with clinical improvement during mycophenolate treatment in systemic sclerosis. J Invest Dermatol. 2013 Aug; 133(8):1979-1989.
4. Skaug B, Khanna D, Swindell WR, Hinchcliff ME, Frech TM, Steen VD, et al. Global skin gene expression analysis of early diffuse cutaneous systemic sclerosis shows a prominent innate and adaptive inflammatory profile. Ann Rheum Dis. 2020 Mar; 79(3):379-386.
5. Piyadasa H, Lloyd D, Lee AHY, Altieri A, Hemshekhar M, Osawa N, et al. Characterization of immune responses and the lung transcriptome in a murine model of IL-33 challenge. Biochim Biophys Acta Mol Basis Dis. 2020 Dec 1; 1866(12):165950.
6. Windhager J, Bodenmiller B, Eling N. An end-to-end workflow for multiplexed image processing and analysis. 2021:2021.2011.2012.468357.
7. Righelli D, Weber LM, Crowell HL, Pardo B, Collado-Torres L, Ghazanfar S, et al. SpatialExperiment: infrastructure for spatially-resolved transcriptomics data in R using Bioconductor. Bioinformatics. 2022; 38(11):3128-3131.
8. Eling N, Damond N, Hoch T, Bodenmiller B. cytomapper: an R/Bioconductor package for visualization of highly multiplexed imaging data. Bioinformatics. 2020; 36(24):5706-5708.
9. Huang J, Beyer C, Palumbo-Zerr K, Zhang Y, Ramming A, Distler A, et al. Nintedanib inhibits fibroblast activation and ameliorates fibrosis in preclinical models of systemic sclerosis. Ann Rheum Dis. 2016 May; 75(5):883-890.
10. Zhou X, Trinh-Minh T, Matei AE, Gyorfi AH, Hong X, Bergmann C, et al. Amelioration of Fibrotic Remodeling of Human 3-Dimensional Full-Thickness Skin by Transglutamase 2 Inhibition. Arthritis Rheumatol. 2023 Sep; 75(9):1619-1627.
11. Zerr P, Distler A, Palumbo-Zerr K, Tomcik M, Vollath S, Dees C, et al. Combined inhibition of c-Abl and PDGF receptors for prevention and treatment of murine sclerodermatous chronic graft-versus-host disease. Am J Pathol. 2012 Nov; 181(5):1672-1680.

12. Zerr P, Palumbo-Zerr K, Distler A, Tomcik M, Vollath S, Munoz LE, et al. Inhibition of hedgehog signaling for the treatment of murine sclerodermatous chronic graft-versus-host disease. Blood. 2012 Oct 4; 120(14):2909-2917.
13. Palumbo-Zerr K, Zerr P, Distler A, Fliehr J, Mancuso R, Huang J, et al. Orphan nuclear receptor NR4A1 regulates transforming growth factor-beta signaling and fibrosis. Nat Med. 2015 Feb; 21(2):150-158.
14. Wohlfahrt T, Rauber S, Uebe S, Luber M, Soare A, Ekici A, et al. PU.1 controls fibroblast polarization and tissue fibrosis. Nature. 2019 Feb; 566(7744):344-349.
15. Bergmann C, Brandt A, Merlevede B, Hallenberger L, Dees C, Wohlfahrt T, et al. The histone demethylase Jumonji domain-containing protein 3 (JMJD3) regulates fibroblast activation in systemic sclerosis. Annals of the rheumatic diseases. 2018 Jan; 77(1):150-158.
16. Yoshizaki A, Yanaba K, Ogawa A, Asano Y, Kadono T, Sato S. Immunization with DNA topoisomerase I and Freund's complete adjuvant induces skin and lung fibrosis and autoimmunity via interleukin-6 signaling. Arthritis and rheumatism. 2011 Nov; 63(11):3575-3585.
17. Zhang Y, Shen L, Dreissigacker K, Zhu H, Trinh-Minh T, Meng X, et al. Targeting of canonical WNT signaling ameliorates experimental sclerodermatous chronic graft-versus-host disease. Blood. 2021 Apr 29; 137(17):2403-2416.
18. Dees C, Potter S, Zhang Y, Bergmann C, Zhou X, Luber M, et al. TGF-beta-induced epigenetic deregulation of SOCS3 facilitates STAT3 signaling to promote fibrosis. J Clin Invest. 2020 May 1; 130(5):2347-2363.
19. Chakraborty D, Zhu H, Jungel A, Summa L, Li YN, Matei AE, et al. Fibroblast growth factor receptor 3 activates a network of profibrotic signaling pathways to promote fibrosis in systemic sclerosis. Sci Transl Med. 2020 Sep 30; 12(563).
20. Ashcroft T, Simpson JM, Timbrell V. Simple method of estimating severity of pulmonary fibrosis on a numerical scale. Journal of clinical pathology. 1988 Apr; 41(4):467-470.
21. Gyorfi AH, Matei AE, Fuchs M, Liang C, Rigau AR, Hong X, et al. Engrailed 1 coordinates cytoskeletal reorganization to induce myofibroblast differentiation. J Exp Med. 2021 Sep 6; 218(9).
22. Zehender A, Li YN, Lin NY, Stefanica A, Nuchel J, Chen CW, et al. TGFbeta promotes fibrosis by MYST1-dependent epigenetic regulation of autophagy. Nat Commun. 2021 Jul 20; 12(1):4404.
23. Zehender A, Huang J, Gyorfi AH, Matei AE, Trinh-Minh T, Xu X, et al. The tyrosine phosphatase SHP2 controls TGFbeta-induced STAT3 signaling to regulate fibroblast activation and fibrosis. Nat Commun. 2018 Aug 14; 9(1):3259.
24. Dees C, Akhmetshina A, Zerr P, Reich N, Palumbo K, Horn A, et al. Platelet-derived serotonin links vascular disease and tissue fibrosis. J Exp Med. 2011 May 9; 208(5):961-972.
25. Akhmetshina A, Palumbo K, Dees C, Bergmann C, Venalis P, Zerr P, et al. Activation of canonical Wnt signalling is required for TGF-beta-mediated fibrosis. Nat Commun. 2012 Mar 13; 3:735.